Fine structure dips in the fission fragment mass distribution for the ^{238}U(^{18}O,f) reaction

L. S. Danu,[1] D. C. Biswas,[1,*] A. Saxena,[1] A. Shrivastava,[1] A. Chatterjee,[1] B. K. Nayak,[1] R. G. Thomas,[1] R. K. Choudhury,[1] R. Palit,[2] I. Mazumdar,[2] P. Datta,[3,†] S. Chattopadhyay,[4] S. Pal,[4] S. Bhattacharya,[5] S. Muralithar,[6] K. S. Golda,[6] R. K. Bhowmik,[6] J. J. Das,[6] R. P. Singh,[6] N. Madhavan,[6] J. Gerl,[7] S. K. Patra,[8] and L. Satpathy[8]

[1]*Nuclear Physics Division, Bhabha Atomic Research Centre, Mumbai 400085, India*

[2]*Tata Institute of Fundamental Research, Mumbai 400005, India*

[3]*Ananda Mohan College, Kolkata 700009, India*

[4]*Saha Institute of Nuclear Physics, Kolkata 400064, India*

[5]*Variable Energy Cyclotron Centre, Kolkata 400064, India*

[6]*Inter University Accelerator Centre, New Delhi 110067, India*

[7]*GSI, Darmstadt, Germany*

[8]*Institute of Physics, Bhubaneswar 751005, India*

(Received 18 August 2009; revised manuscript received 19 November 2009; published 22 January 2010)

Fission fragment mass distribution has been determined in the ^{238}U(^{18}O,f) reaction from the on-line measurement of individual even-even fragment yields by analyzing the γ-γ matrix. Fine structure dips corresponding to fragment shell closures at $Z = 50$ and $N = 82$ are observed, indicating the effect of nuclear structure in the dynamical evolution of fissioning nucleus. The present results may suggest a new feature of shape inhibition of closed shell nuclei at the scission point.

DOI: 10.1103/PhysRevC.81.014311 PACS number(s): 25.70.Jj, 24.75.+i, 25.85.Ge, 29.30.Kv

I. INTRODUCTION

Nuclear fission is a complex process involving large scale collective rearrangement of nuclear matter. The shape of the fissioning nucleus evolves in the multidimensional space of relative separation, neck opening, mass asymmetry, and deformation of the fragments [1]. The fission fragment mass and charge distributions are decided during saddle to scission transition and are related to the scission configuration. Various models have been put forward to describe the fission fragment mass distribution as well as the shapes of the fragments at scission [1–4]. Conventionally, fission fragment mass distribution has been studied by measuring the energy and/or the time of flight of the correlated fission fragments [5–8]. One of the limitations of these measurements is that one can only achieve mass resolution of 4–5 units. On the contrary, by carrying out fission fragment spectroscopy employing the γ-γ coincidence technique, it is possible to identify the individual fission fragments [9,10]. The spectroscopic studies of fission fragments also provide direct information on the nuclear excited states, which are related to the shape and structure of the fragment nuclei [11,12].

Detailed fission fragment mass distribution studies provide an opportunity to explore the interplay of the structure and dynamics in the fission process [13]. Fragment mass distributions have been reported earlier from the study of fission fragment spectroscopy in various fissioning systems [14,15]. The recent results on fragment mass distribution in ^{18}O + ^{208}Pb reaction [16], show overall good agreement of the mass width with that obtained by other techniques [17]. However, the mass yield distribution in this system showed fine structure dips for certain masses, which was not explained due to the lack of systematic information on the fragment yields. In the present work, we report the results on fission fragment mass distribution in ^{238}U(^{18}O,f) reaction measured from the γ-γ coincidence matrix. Similar features of fine structure dips are observed in the fragment mass distribution for both ^{238}U,^{208}Pb(^{18}O,f) reactions, implying some common underlying effect of microscopic structure of the fragments on the mass yields.

II. EXPERIMENTAL DETAILS AND DATA ANALYSIS

The present experiment was carried out at the 15UD IUAC Pelletron accelerator facility, New Delhi, using ^{18}O beam of energy 100 MeV to bombard a self-supporting ^{238}U target of thickness $\sim$15 mg/cm^2. The Coulomb barrier of the reaction is 87.7 MeV (in the laboratory frame) and the fusion cross section at 100 MeV is 540 mb, as obtained from the CCFUS calculation [18]. The beam energy loss in the target is about 23 MeV and at the outgoing energy, the fusion cross section is 0.05 mb, which is negligibly small. The maximum excitation energy of the compound nucleus, ^{256}Fm is $E^* = 54$ MeV. Most of the fusion-fission reaction takes place in the first half of the target and the range of the fission fragments produced in this reaction is less than the half-thickness of the ^{238}U target. Thus, in the present setup, at least one of the fragments gets stopped in the target, thereby reducing the Doppler broadening effect on the energy of γ rays. The γ rays emitted by the fission fragments were detected using the Indian National Gamma Array (INGA) comprised of 18 Compton suppressed Clover detectors, each having an intrinsic photopeak efficiency $\sim$0.2% [19]. The clover detectors were mounted at a distance of 24 cm from the target with the accompanying anti-Compton

*dcbiswas@barc.gov.in

†Present address: Department of Nuclear Physics, iThemba Labs, South Africa.

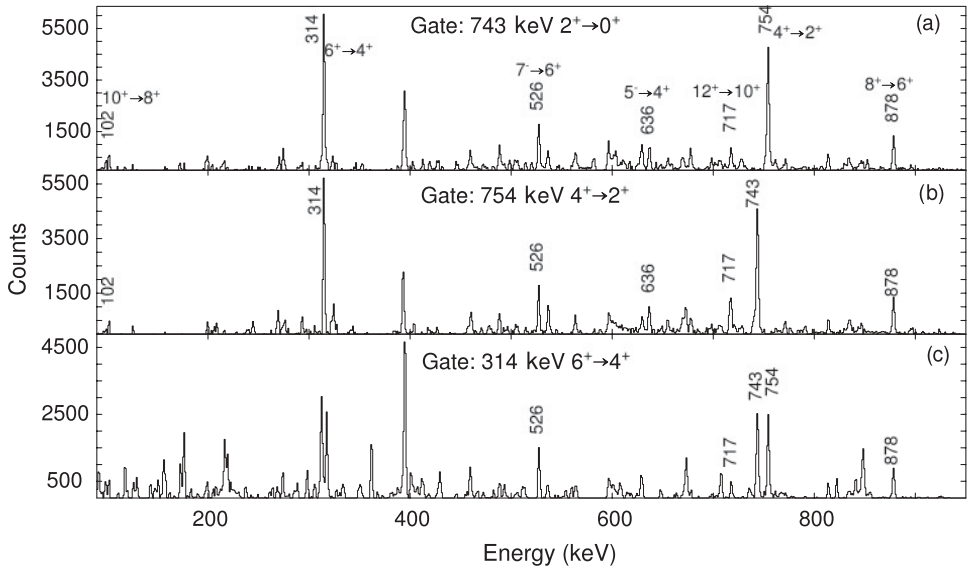

FIG. 1. γ-ray energy spectra obtained with gates on (a) $2^+ \rightarrow 0^+$ ($E_\gamma = 743$ keV), (b) $4^+ \rightarrow 2^+$ ($E_\gamma = 754$ keV), and (c) $6^+ \rightarrow 4^+$ ($E_\gamma = 314$ keV) ground-state transitions of ^{128}Te. The labeled lines belong to ^{128}Te and some of the unlabeled lines are due to complementary fragments and contamination from other fragments.

shields. These detectors were arranged in five rings viz., 32°, 57°, 90°, 123°, and 148° with respect to the beam direction and each detector subtends an opening angle of 29° at the target center. A Hit Pattern based data collection was done by using the CANDLE software [20]. The Compton suppressed data were collected in an event-by-event mode with the minimum requirement of threefold prompt γ-ray coincidence, for which the event rate was 1.6 K/s with the beam current ~3 pnA. The coincidence time gate for recording the data was set at about 350 ns. The overall energy resolution in the total projection spectrum of the γ rays was found to be about 1.8 keV at $E_\gamma =$ 200 keV.

In the data analysis, a total of $\sim 1.9 \times 10^8$ threefold events have been considered and the E_γ-E_γ matrix is constructed from the prompt γ-ray coincidence data. The data were analyzed using RADWARE software [21] to obtain the independent yields of the fission fragments. As an example of the quality of the data, the γ-energy spectra gated on the $2^+ \rightarrow 0^+$ ($E_\gamma = 743$ keV), $4^+ \rightarrow 2^+$ ($E_\gamma = 754$ keV), and $6^+ \rightarrow 4^+$ ($E_\gamma = 314$ keV) ground state (g.s.) transitions for ^{128}Te are shown in Fig. 1. In this figure we have labeled only the transitions belonging to ^{128}Te. Some of the unlabeled lines belong to complementary fragments of ^{128}Te and there are a few peaks that appear as backgrounds due to some other nuclei produced in nuclear fission. It is also observed from Fig. 1, that the intensity of γ rays for $2^+ \rightarrow 0^+$ and $4^+ \rightarrow 2^+$ transitions are almost equal for the gate on the $6^+ \rightarrow 4^+$ ($E_\gamma = 314$ keV) transition, implying sequential cascade decays from a given fragment. The total intensities of the $2^+ \rightarrow 0^+$ and $4^+ \rightarrow 2^+$ transitions observed in the de-excitation of even-even fission products provide to a high degree of accuracy, the yield of the fragment isotopes [9,10]. In the present work, the independent yield of a particular fragment nucleus has been determined from the coincidence of γ rays of $2^+ \rightarrow 0^+$ and $4^+ \rightarrow 2^+$ transitions. For some of the nuclei, the γ rays of $2^+ \rightarrow 0^+$ and $4^+ \rightarrow 2^+$ transitions are very close in energy and in such cases their relative yield was determined by gating on higher transitions. The yields of several even-even isotopes, $^{90-96}$Sr, $^{96-102}$Zr, $^{98-108}$Mo, $^{104-112}$Ru, $^{108-116}$Pd, $^{114-122}$Cd, $^{116-128}$Sn, $^{124-134}$Te, $^{130-138}$Xe, $^{136-144}$Ba, $^{142-148}$Ce, $^{146-152}$Nd, and $^{150-158}$Sm have been determined from the γ-γ coincidence matrix.

In compound nuclear fission at this excitation energy, light charged particles (proton and alpha) are also emitted and their cross section is less than 1% [22]. Thus, their contribution to the total fission yield is negligible as compared to the binary fission along with neutron emission, and the total charge is conserved for the correlated fragments. In Fig. 2, we have plotted the relative yield distribution of correlated fragments (Sr-Sm, Zr-Nd, Mo-Ce, Ru-Ba, Pd-Xe, Cd-Te, and Sn-Sn isotopes) produced in the reaction. It is observed that the isotopic yield of the fragments follows a bell-shape distribution, which implies that the yield of a particular fragment depends on the N/Z ratio. From the correlated yield distribution, it is also found that 8–10 neutron emission channels have dominating yields and in the case of Sn-Sn pair, the $12n$ emission channel has maximum yield. In fission reactions, neutrons are emitted both in pre- and post-scission stages during the decay of the compound nucleus to fission fragments. In the case of the Sn-Sn fragment pair, a relatively larger number of neutron emission implies a fissioning nucleus of lower excitation energy, which may lead to a reduction in the fission probability. However, we will discuss the results on the fission fragment yields in more detail in the following section.

III. RESULTS AND DISCUSSIONS

The fission fragment mass distribution is obtained by adding the yields of various nuclei corresponding to a particular mass as shown in Fig. 3(a). It is found that the fragment mass distribution is symmetric about ^{124}Sn (half of the compound nuclear mass is $A_{CN}/2 = 128$ and the missing mass is due to the evaporation of neutrons). We also observe some dips in the mass distribution, corresponding to fragment masses $A = 112$, 124, and 136, where the yield is significantly reduced. In an earlier measurement, Bogachev *et al.* reported the mass

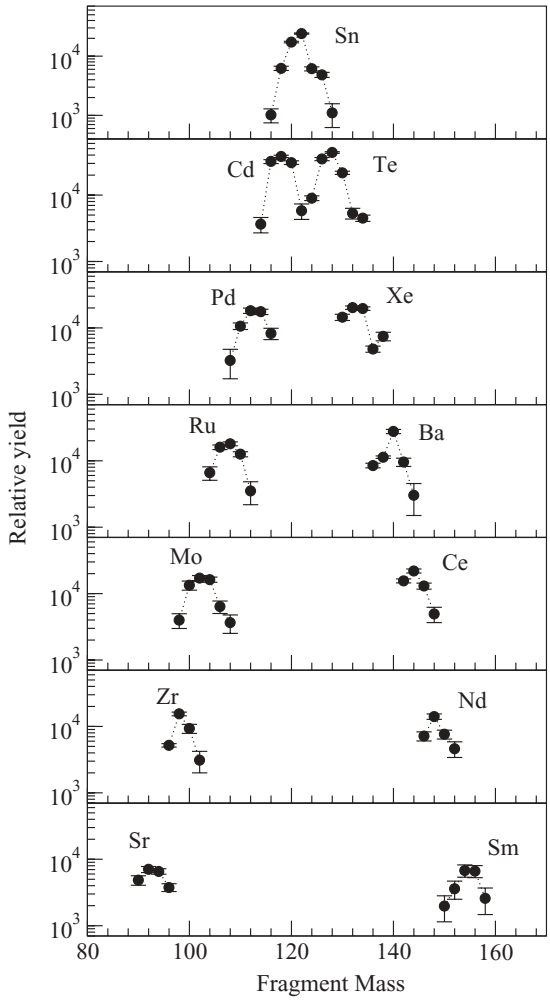

FIG. 2. Relative yield distribution of various fission fragments produced in $^{18}O + ^{238}U$ reaction at 100 MeV. The dotted lines are to guide the eye.

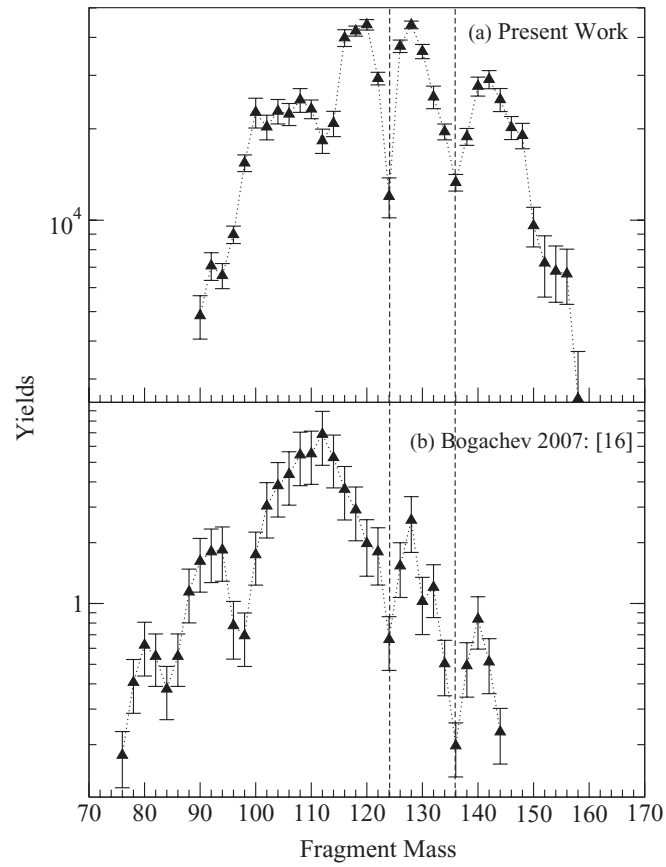

FIG. 3. Fission fragment mass distribution obtained in (a) $^{18}O + ^{238}U$ at 100 MeV (present work) and (b) $^{18}O + ^{208}Pb$ at 85 MeV [16].

distribution of the fission fragments for the $^{208}Pb(^{18}O, f)$ reaction at 85 MeV from the γ-ray spectroscopy studies [16]. An overall symmetric mass distribution peaking at a value near half of the compound nuclear mass, $A_{CN}/2 = 112$ was observed. The mass distribution showed dips (at $A = 84$, 98, 124, and 136) and these data are also plotted in Fig. 3(b). Comparing the mass distributions for $^{238}U,^{208}Pb(^{18}O, f)$ reactions, it is observed that the dips at the closed shell nuclei for $A = 124$ ($Z = 50$ shell) and for $A = 136$ ($N = 82$ shell) are seen in both cases. The other dips at $A = 112$ in the present work and at $A = 84$ and 98 for the ^{208}Pb ($^{18}O, f$) system [16], are due to the complementary fragment masses of $A = 124$ and 136. It is most likely that the structures/dips in the mass distribution appear because of these $A = 124$ and 136 closed shell nuclei.

The dips observed in the mass distribution at $A = 124$ and 136 (closed shell nuclei) can be partly accounted for, due to the presence of isomeric states. Some of the nuclei in these mass regions have long-lived isomeric states, e.g., ^{124}Sn (10^+ state, $T_{\frac{1}{2}} = 45$ s and 7^- state $T_{\frac{1}{2}} = 0.36$ s), ^{136}Xe (6^+ state, $T_{\frac{1}{2}} = 2.95$ μs), ^{136}Ba (7^- lifetime, $T_{\frac{1}{2}} = 0.304$ s). Many of these nuclei which are populated above these isomeric states will not decay to ground state within the time gate of the data acquisition. These isomeric states will cause a reduction in the intensity of $2^+ \rightarrow 0^+$ and $4^+ \rightarrow 2^+$ γ-ray transitions and will lead to an underestimation of the fragment yields. In the present analysis, the effect of long-lived isomeric states has been corrected from the known lifetime and intensity data; except for the Sn isotopes due to the lack of detailed spectroscopic information. For example, the 6^+ state in ^{136}Xe has a half-life 2.95 μs and due to this, the intensity of the $6^+ \rightarrow 4^+$ transition is reduced by a factor of 3.5, which has been estimated by analyzing the coincidence data above and below this state. In a similar way, we have also incorporated the contribution due to the isomeric states in ^{136}Ba. In some nuclei, the sidebands directly feeding to the 2^+ state of the g.s. band are populated with significant intensity and their contribution is excluded in the yield determination, if we consider only coincidence between $2^+ \rightarrow 0^+$ and $4^+ \rightarrow 2^+$ transitions. For example, in ^{96}Zr we observe that the 2^+ state of the g.s. band is fed by the 3^- state sideband with significant intensity. The yield determination has been carried out from the coincidence of $2^+ \rightarrow 0^+$ and $4^+ \rightarrow 2^+$ of the g.s. as well as $2^+ \rightarrow 0^+$ g.s. and $3^- \rightarrow 2^+$ sideband transitions. Similarly, the yields of ^{98}Zr, ^{100}Mo, $^{108-116}Pd$, etc., have also been corrected for the contribution of the side-feeding.

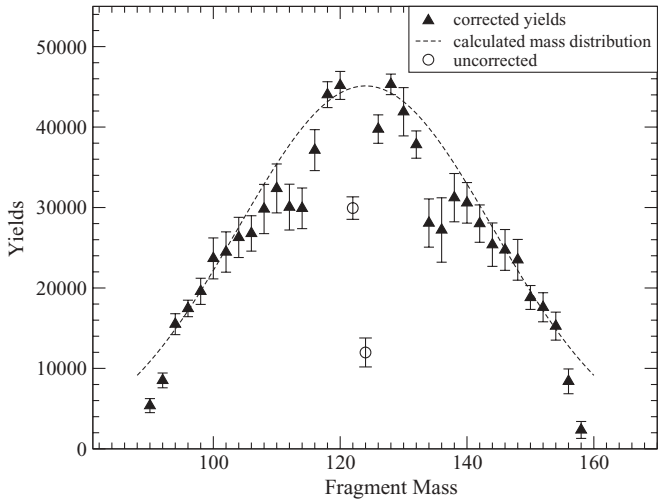

FIG. 4. Fission fragment mass distribution of various fission fragments produced in $^{18}O + ^{238}U$ along with the calculations, using mass width systematics of $^{16}O + ^{238}U$ [6], see text.

After incorporating the above corrections the mass distribution obtained for the even-even fragments is shown in Fig. 4. It is seen that even after correcting for the isomeric and side-feeding effects, the dips at $A = 136$ and its complementary fragment ($A = 112$) still persist. These results indicate the reduced production of ^{136}Xe as well as ^{136}Ba fragments, near the neutron shell closure ($N = 82$). Accordingly, the yield of $A = 112$ is also less since it is complementary to $A = 136$. A similar conclusion may also be drawn for the case of $A = 124$ ($Z = 50$) fragments, although we have not carried out the corresponding corrections for the isomeric states in this case. The average behavior of the mass distribution is found to be in agreement with the systematics of the energy dependent mass width measured for the $^{16}O + ^{238}U$ system [6]. The calculations were done by taking the weighted average of the mass distributions over the energy range from the cross sections obtained using the CCFUS code [18]. The width of the theoretically calculated mass distribution is obtained to be about $\sigma_M \approx 20.5$ amu, which compares well with the overall experimental mass distribution as shown by the dashed line in Fig. 4.

The reduction in the yields for closed shell nuclei could also be due to the variations in the level density with the fragment mass. This will cause a change in the neutron-evaporation widths for the fission fragments at the shell closure and will influence the fission fragment mass distribution. However, from the results of Bogachev *et al.* and the present work, it is observed that irrespective of the compound system, the dips in the fragment mass yields occur for $A = 124$ and 136 and their complementary fragments. This is a new feature and may be explained if one invokes 'shape inhibition' of the closed shell nuclei in the fission process. This can be visualized from the shape evolution of the compound nucleus from the saddle to scission configuration. When the fissioning nucleus evolves toward an elongated shape for undergoing fission and if one of the fission fragment partners has the closed shell configuration, its contribution to fission gets reduced as it has to overcome relatively higher barrier in the multidimensional potential energy surface. Since in the composite system, the partner having closed shell configuration cannot be easily deformed, only the complementary partner has to attain larger deformation for moving toward the scission configuration. In the fission fragment mass distribution, the yield corresponding to these mass channels is thus expected to be less. In the present work, the dip at $A = 136$ is related to the $N = 82$ shell closure of the heavy fragment. Again, for the symmetric split in $^{18}O + ^{238}U$ system, where the Sn-Sn correlated fragments are formed, the proton closed shell ($Z = 50$) fragment production probability will be much smaller because of a similar hindrance due to the shape inhibition. In this case the reduction is twofold as both the fragments have compact shape and will see a very large potential barrier during the shape evolution. Although there are theoretical model calculations to understand the fission yield distribution, the role of shell structure of the fragments on the mass distribution has not been fully understood and more investigations are required to explain these results [1,2].

IV. SUMMARY

In summary, the fission fragment yield distribution in the ^{238}U ($^{18}O, f$) system has been measured by employing the γ-γ coincidence technique. The mass distribution is found to be symmetric around $A = 124$, corresponding to an average of eight neutrons evaporated from the compound nucleus and the excited fission fragments. The fitted mass distribution, shown by the dashed line in Fig. 4, is symmetric with an overall width of $\sigma_M = 20.5$ amu, which is similar to other heavy systems obtained by employing the time of flight technique [5,6]. Fine structure dips are observed in the mass distribution, which seem to be related to the shell closure of the individual fission fragment nuclei for $Z = 50$ and $N = 82$ shells, where the yields are depleted. Similar fine structure dips have been observed Bogachev *et al.* in the $^{18}O + ^{208}Pb$ system. In both these experiments, there is a clear indication of nuclear structure effects in the fission fragment mass distribution. We interpret the fine structure dips in the mass yields to be due to "shape inhibition" of close shell fragment nuclei at the scission point. The present results provide important new insight into the understanding of the dynamical behavior fragment formation in the fission process. More systematic experimental data as well as theoretical calculations will be required to clearly understand these experimental observations.

ACKNOWLEDGMENTS

The authors are thankful to Dr. S. S. Kapoor, Dr. S. Kailas, and Dr. Amit Roy for their suggestions to and encouragement of this work. We acknowledge the support and help of the Pelletron operation staff and Electronics group of IUAC, New Delhi. We also thank T. Trivedi, G. Jnaneswari, D. Negi, and Kumar Raju for their contribution during the experiment.

[1] P. Möller and A. Iwamoto, Phys. Rev. C **61**, 047602 (2000).
[2] U. Brosa, S. Grossmann, and A. Muller, Phys. Rep. **197**, 167 (1990); J. Benlliure, A. Grewe, M. de Jong, K.-H. Schmidt, and S. Zhdanov, Nucl. Phys. **A628**, 458 (1998).
[3] P. A. Butler and W. Nazarewicz, Nucl. Phys A **533**, 249 (1991); Rev. Mod. Phys. **68**, 349 (1996).
[4] L. Satpathy and S. K. Patra, J. Phys. G: Nucl. Part. Phys. **30**, 771 (2004).
[5] T. K. Ghosh *et al.*, Phys. Rev. C **69**, 031603(R) (2004); **70**, 011604(R) (2004).
[6] R. Yanez, D. J. Hinde, B. Bouriquet, and D. Duniec, Phys. Rev. C **71**, 041602(R) (2005).
[7] L. M. Pant, R. K. Choudhury, A. Saxena, and D. C. Biswas, Eur. Phys. J. A **11**, 47 (2001)
[8] Y. Sawant A. Saxena, R. K. Choudhury, P. K. Sahu, R. G. Thomas, L. M. Pant, B. K. Nayak, and D. C. Biswas, Phys. Rev. C **70**, 051602(R) (2004).
[9] G. M. Ter-Akopian *et al.*, Phys. Rev. Lett. **77**, 32 (1996).
[10] D. C. Biswas *et al.*, Eur. Phys. J. A **7**, 189 (2000).
[11] A. G. Smith *et al.*, Phys. Rev. Lett. **77**, 1711 (1996).
[12] D. C. Biswas *et al.*, Phys. Rev. C **71**, 011301(R) (2005).
[13] K.-H. Schmidt, J. Benlliure, and A. R. Junghans, Nucl. Phys. **A693**, 169 (2001).
[14] N. Fotiades *et al.*, Phys. Rev. C **67**, 034602 (2003).
[15] C. Y. Wu *et al.*, Phys. Rev. C **73**, 034312 (2006).
[16] A. Bogachev *et al.*, Eur. Phys. J. A **34**, 23 (2007).
[17] I. V. Pokrovsky *et al.*, Phys. Rev. C **62**, 014615 (2000); G. Chubarian *et al.*, Phys. Rev. Lett. **87**, 052701 (2001).
[18] J. Fernandez-Niello, C. H. Dasso, and S. Landowne, Comput. Phys. Commun. **54**, 409 (1989).
[19] S. Muralithar *et al.*, DAE Symposium on Nucl. Phys. **53**, 689 (2008).
[20] E. T. Subramaniam *et al.*, Rev. Sci. Instrum. **77**, 096102 (2006).
[21] D. C. Radford, Nucl. Instrum. Methods Phys. Res. A **361**, 297 (1995).
[22] A. Chatterjee, A. Navin, S. Kailas, P. Singh, D. C. Biswas, A. Karnik, and S. S. Kapoor, Phys. Rev. C **52**, 3167 (1995).